PHASED SUBARRAY IMAGING FOR LOW-COST, WIDEBAND COHERENT ARRAY IMAGING

Jeremy A. Johnson[a], Ömer Oralkan[a], A. Sanlı Ergun[a], Utkan Demirci[a], Mustafa Karaman[b], Butrus T. Khuri-Yakub[a]

[a] E. L. Ginzton Laboratories, Stanford University, Stanford, CA, USA
[b] Işık University, Department of Electronics Engineering, Istanbul, Turkey

Abstract—**The front-end hardware complexity of conventional full phased array (FPA) imaging is proportional to the number of array elements. Phased subarray (PSA) imaging has been proposed as a method of reducing the hardware complexity—and therefore system cost and size—while achieving near-FPA image quality. A new method is presented for designing the subarray-dependent interpolation filters suitable for wideband PSA imaging. The method was tested experimentally using pulse-echo data of a wire target phantom acquired using a 3.2-cm, 128-element capacitive micromachined ultrasonic transducer (CMUT) array with 85% fractional bandwidth at 3 MHz. A specific PSA configuration using seven 32-element subarrays was compared to FPA imaging, representing a 4-fold reduction in front-end hardware complexity and a 43% decrease in frame rate. For targets near the fixed transmit focal distance, the mean 6-dB lateral resolution was identical to that of FPA, the axial resolution improved by 4%, and the SNR decreased by 5 dB. Measurements were repeated for 10 different PSA configurations with subarray sizes ranging from 4 to 60. The lateral and axial resolutions did not vary significantly with subarray size; both the SNR and contrast-to-noise ratio (CNR) improved with increased subarray size.**

I. INTRODUCTION

Conventional phased array imaging systems simultaneously transmit on and receive from all transducer elements to form each beam of a sector image. We refer to this method as full phased array (FPA) imaging. This architecture requires that each element have a dedicated front-end electronic channel for pulse transmission, received signal amplification, filtering, time-gain compensation, and analog-to-digital conversion. The number of front-end channels—or front-end hardware complexity—directly affects the size and cost of the system [1]. For size- and cost-constrained phased array imaging systems, it may not be possible to employ a full set of front-end channels. This restriction is especially evident for 3D phased array imaging using fully-populated 2D arrays.

Phased subarray imaging has been proposed as a method of reducing the front-end hardware complexity while maintaining high image quality [2, 3]. The full array is subdivided into a number of overlapping subarrays. The number of front-end channels required is equal to the size of the subarrays. A small number of beams—as determined by the Nyquist sampling criteria—are acquired consecutively from each of the subarrays. These low-resolution subarray images are laterally upsampled, interpolated, weighted, and coherently summed to form the final FPA-equivalent high-resolution image.

In previous studies, a lateral 1D interpolation filter was used to reconstruct the low-resolution subarray images. Although the 1D filter is suitable for narrowband imaging, a 2D filter with support in both the lateral and axial dimensions is required when applied to wideband systems.

This paper outlines a new method of designing the subarray-dependent interpolation filters for wideband PSA imaging. The flexibility of the method is verified experimentally for several different subarray sizes. Readers interested in a more detailed treatment of the methods and results presented here are referred to [4].

II. METHODS

A. Experimental Data

Experimental A-scans were acquired using a 128-element linear CMUT array with an element pitch of 250 µm and height of 6 mm. The array was biased with 40 V DC, and transmit excitation was generated with a 15-V, 100-ns unipolar pulse. The received signals were amplified by 60 dB, sampled at 50 MHz,

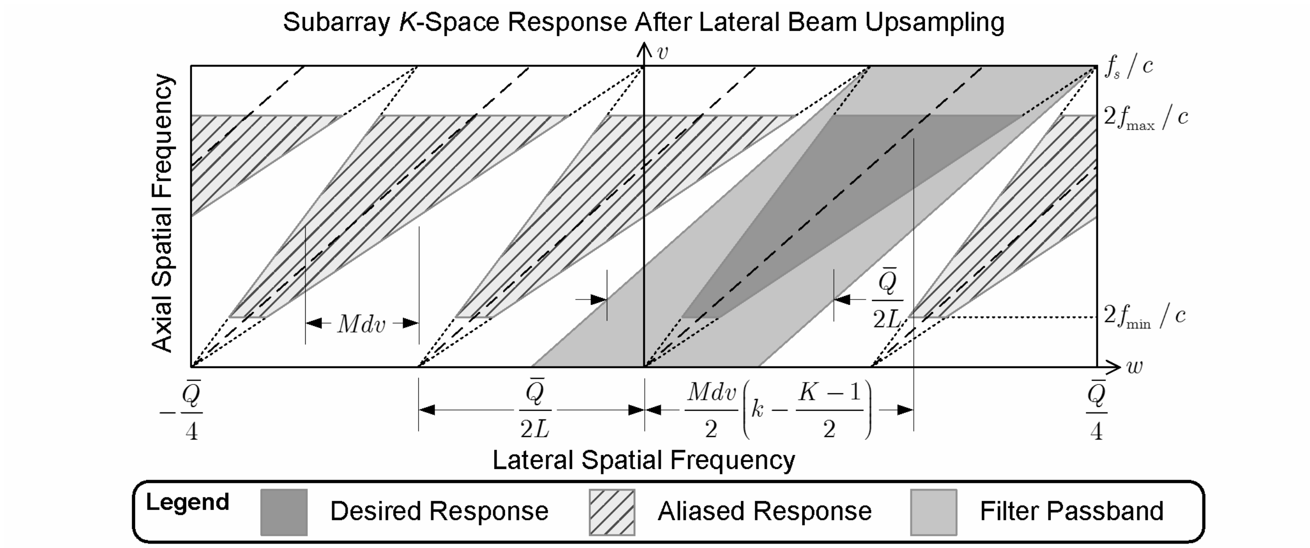

Figure 1. Spatial frequency response of a single subarray after beam upsampling and before reconstruction filtering. The dimensions are given for the general case; the passband regions shown correspond to an off-center subarray and an upsampling rate of L=4.

and filtered with a 1–5 MHz digital bandpass filter. A-scans were acquired for all transmit and receive element combinations.

Parallel steel wires (0.38 mm diameter) submerged in an oil bath were used as an imaging phantom. A typical A-scan had a center frequency response of 3.0 MHz, and a 6-dB fractional bandwidth of 80% without attenuation or diffraction compensation. A more detailed description of the array and acquisition system is given in [5].

B. Beamformer

Custom software applied synthetic phased array beamforming to the A-cans to generate beam samples for all imaging methods. Delay-and-sum beamforming was employed with a fixed transmit focus at 13.1 cm (the depth of the 4th target) and dynamic receive focusing. The temporal beamsampling rate was 12 MHz. All beams emanated from the center of the array and were uniformly spaced in $\sin\theta$, where θ is measured from the array normal.

For FPA imaging, data from all 128 elements was used to form 361 beams over a 90° sector angle. These beams formed the final FPA image.

For PSA imaging, one set of 91 beams was formed for each of the seven subarrays, resulting in a total of 637 beams for a single image frame. Only the A-scans corresponding to the 32 active subarray elements were used to form each of these low-resolution images.

C. Phased Subarray Image Formation

The low-resolution subarray images were digitally processed to form the final PSA image. The first step was to laterally upsample by a factor of four, equivalent to inserting three zero-sampled beams between each of the 91 acquired beams. Next, a 2D finite impulse response (FIR) filter designed for each subarray was convolved with the upsampled images. These high-resolution subarray images were then coherently summed, resulting in the final PSA image.

D. Interpolation Filter Design

The purpose of the interpolation filters is to reconstruct the high-resolution subarray images given the subset of beams that form the low-resolution subarray images. In the spatial domain, this corresponds to estimating the zero-valued beam samples between the acquired beams. In the spatial frequency domain, or *k*-space [6], the filters are designed to suppress the aliases that result from upsampling while simultaneously preserving the desired response.

Figure 1 illustrates the role of the interpolation filter in *k*-space. The notation used in this figure is as follows: v and w are the axial and lateral spatial frequency coordinates, respectively; f_s is the temporal beam sampling rate; $f_{\min}$ and $f_{\max}$ are the minimum and maximum frequency components of the system impulse response; c is the velocity of sound; M is the number of elements in each subarray; L is the upsampling rate; d is the element pitch; K is the number of subarrays; k is the subarray index in the

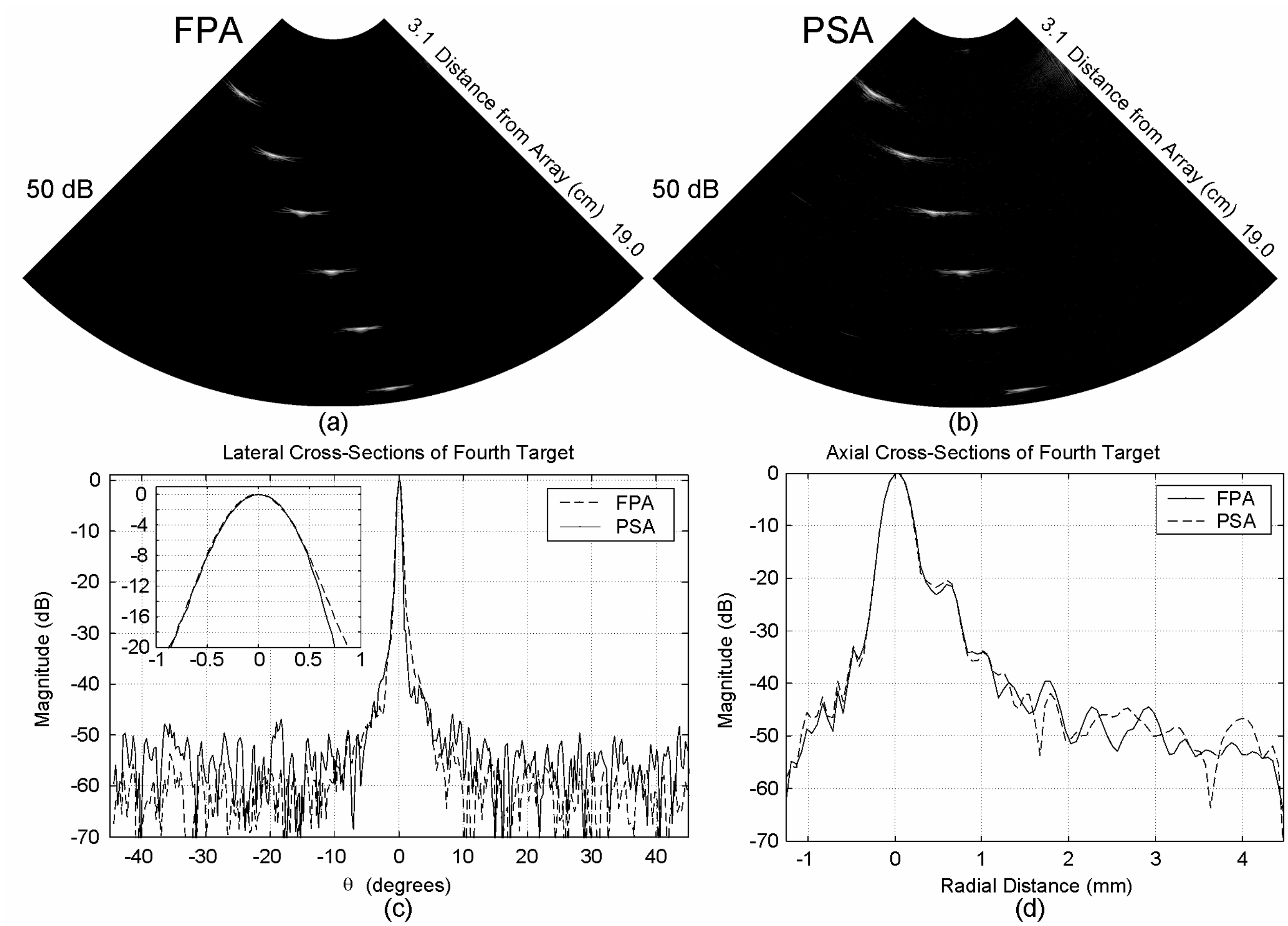

Figure 2. Comparison of experimental wire target images formed by conventional FPA imaging and PSA imaging using wideband reconstruction filters. A 128-element CMUT array was used. The PSA configuration consisted of 32 front-end channels, reducing the front-end hardware complexity by a factor of 4.

range $(0, K-1)$; and $\bar{Q} = Q/\sin(\Theta/2)$, where Q is the number of beams and Θ is the sector scan angle.

For each subarray, the filter was defined as a 2D passband region in *k*-space:

$$H_k(v,w) = \begin{cases} 1, & \left| w - \frac{Mdv}{2}\left(k - \frac{K-1}{2}\right) \right| < \frac{\bar{Q}}{4L} \\ 0, & \text{otherwise} \end{cases} \quad (1)$$

An example passband is illustrated in Figure 1 for an off-center subarray. The spatial filter kernels were calculated by applying the Fourier transform, truncating to 31 taps in both dimensions, and multiplying by a Hamming window.

III. RESULTS

A PSA image formed using 32-element subarrays is compared to the corresponding FPA image in Figures 2(a) and (b). Both images are displayed with 50 dB of logarithmic compression. The primary differences are slightly wider point responses and a slight increase in background noise in the PSA image compared to the FPA image. The lateral cross-sections through the images at the location of the 4th target have similar shape for the two methods, as shown in Figure 2(c). The PSA cross-section has a slightly higher noise floor. The axial cross-sections for the two methods are nearly identical, as shown in Figure 2(d).

A summary of the results comparing FPA and PSA imaging is given in Table I. Compared to FPA imaging, this PSA configuration reduces the front-end hardware complexity by a factor of 4. Due to the increased number of beams acquired to form each frame, the frame rate of a real-time implementation of PSA imaging would be reduced by 43% compared to FPA imaging. The lateral and axial resolutions were

TABLE I. PSA RESULTS FOR 32-ELEMENT SUBARRAYS.

Parameter	FPA	PSA	PSA[1]
# of front-end channels	128	32	25%
# of firings per frame	361	637	176%
Frame rate (frames/s)	10	6	57%
6-dB lateral resolution[2] (°)	0.96	0.96	100%
6-dB axial resolution[2] (mm)	0.35	0.33	96%
Image SNR[2] (dB)	63	57	–6
CNR, 4-mm cyst	3.4	3.4	100%
CNR, 8-mm cyst	5.4	4.8	90%

[1] Normalized to FPA. [2] Mean of targets 3-6.

measured as the 6-dB main lobe widths at each point in the image. The SNR was measured as the ratio of the peak intensity to the standard deviation of an area surrounding each point. Averages of these measurements made at the four points nearest the fixed transmit focal point—targets 3 through 6—are given in Table I. There is little change in resolution, and only a 6 dB loss of SNR. Images of simulated 4-mm and 8-mm speckle phantoms were used for CNR measurements [2]. The decreased CNR of the 8-mm cyst indicates that the point-spread function of the PSA system has larger far side lobes than FPA.

To illustrate the flexibility of PSA system design and the effects of subarray size on the imaging performance, measurements were repeated for 10 different PSA system configurations. Only the center 120 transducer elements were used, and the subarray size ranged from 4 to 60 (numbers of subarrays ranged from 59 to 3). The measurements of FPA and for three example PSA configurations are given in Table II. Measurements for all 10 subarrays varied monotonically.

Decreasing the subarray size in order to reduce the number of front-end channels has a number of effects on system and image performance. First, there is an increase in total number of beams acquired for each frame, resulting in reduced frame rate. Compared to FPA, the frame rate is not reduced by more than a factor of two. Second, the lateral resolution improves somewhat, while the axial resolution remains relatively constant. Third, the SNR is reduced with smaller subarray sizes due to reduced total transmit and receive power per frame. Last, the CNR for both cyst sizes decreases. These results demonstrate the tradeoff between hardware complexity and image quality that is made possible with PSA imaging.

TABLE II. EFFECTS OF SUBARRAY SIZE ON IMAGE QUALITY.

	FPA	PSA[1]		
Parameter		*K*=4	*K*=20	*K*=60
# of front-end channels	120	3%	17%	50%
# of firings per frame	339	197%	183%	150%
Frame rate (frames/s)	11	51%	55%	67%
6-dB lateral resolution[2] (°)	1.0	90%	92%	104%
6-dB axial resolution[2] (mm)	0.35	95%	97%	98%
Image SNR[2] (dB)	62	–20	–10	–2
CNR, 4-mm cyst	3.8	80%	97%	104%
CNR, 8-mm cyst	5.3	65%	80%	109%

[1] Normalized to FPA. [2] Mean of targets 3-6.

IV. CONCLUSION

Phased subarray imaging has been demonstrated experimentally using a new reconstruction filter designed for wideband imaging. PSA imaging is a promising alternative to FPA imaging for systems with large numbers of elements, systems constrained by size, or for 3D imaging with 2D transducer arrays.

V. REFERENCES

[1] M. E. Schafer and P. A. Lewin, "The influence of front-end hardware on digital ultrasonic imaging," *IEEE Trans. Sonics Ultrason.*, pp. 295-306, 1984.

[2] M. Karaman and M. O'Donnell, "Subaperture processing for ultrasonic imaging," *IEEE Trans. Ultrason., Ferroelect., Freq. Contr.*, pp. 126-135, 1998.

[3] J. A. Johnson, M. Karaman, and P. Khuri-Yakub, "Image formation and restoration using multi-element synthetic array processing," *Proc. SPIE Int. Soc. Opt. Eng.*, 2002.

[4] J. A. Johnson, "Coherent array imaging using phased subarrays," Ph.D. dissertation, Department of Electrical Engineering, Stanford University, Stanford, CA, 2003.

[5] Ö. Oralkan, A. S. Ergun, J. A. Johnson, M. Karaman, U. Demirci, K. Kaviani, T. H. Lee, and B. T. Khuri-Yakub, "Capacitive micromachined ultrasonic transducers: next-generation arrays for acoustic imaging?," *IEEE Trans. Ultrason., Ferroelect., Freq. Contr.*, vol. 49, pp. 1596-610, 2002.

[6] W. F. Walker and G. E. Trahey, "The application of k-space in pulse echo ultrasound," *IEEE Trans. Ultrason., Ferroelect., Freq. Contr.*, vol. 45, pp. 541-558, 1998.